Jerzy GOŁĘBIOWSKI [1], Arkadiusz ŁUKJANIUK [1], Robert Piotr BYCUL[2]

Bialystok University of Technology (1), Tieto Poland Ltd. (2)

A numeric simulation of transient thermal field in a transistor-radiator system and its verification by measurements

Abstract. A physical and mathematical model of heat transfer in a system of a power transistor and forced air stream cooled radiator was presented. An important part of the model was the estimation of the heat transfer coefficient for forced convection and radiation. Transient thermal field was determined with the use of the finite element method by using a professional computer program NISA v. 16. The results were verified by doing measurements. Thermoelectric sensors of the T type, an NI 9211 module and an NI Signal Express computer program were utilized during the measuring. The relative difference between the results of the computations and the measurements did not exceed 15,5% in the transient state and it dropped to 6% in the steady state.

Streszczenie. W pracy przedstawiono fizyczny i matematyczny model propagacji ciepła w układzie tranzystora mocy i radiatora chłodzonego wentylatorem. Istotnym elementem modelu było oszacowanie współczynnika przejmowania ciepła z układu w warunkach wymuszonej konwekcji i promieniowania. Nieustalone pole termiczne wyznaczono metodą elementów skończonych za pomocą profesjonalnego programu NISA v.16. Wyniki numerycznej symulacji zweryfikowano na drodze pomiarowej. W tym celu wykorzystano termoelektryczne czujniki typu T, moduł NI 9211 oraz oprogramowanie NI Signal Express. Okazało się, że względna różnica między wynikami obliczeń i pomiarów nie przekroczyła w stanie przejściowym 15,5% i w stanie ustalonym zmalała do 6%. (Numeryczna symulacja nieustalonego pola termicznego w układzie tranzystor-radiator i jej pomiarowa weryfikacja)

Keywords: radiator, forced convection, transient thermal field, measurements.
Słowa kluczowe: radiator, konwekcja wymuszona, nieustalone pole termiczne, pomiary.

Introduction

The electric current flowing through a semiconductor element generates heat. The heat has to be dissipated to the ambience by the semiconductor's case for the working temperature may not exceed the critical value, stated by the producer of the element. To increase the maximum load of the element one has to ensure better cooling conditions. For this reason radiators, heat exchangers, fans, heat pipes, Peltier's cells and other solutions are commonly applied in electronic devices. In the present paper a distribution of transient thermal field in a radiator dissipating heat from a bipolar power transistor BD901 (Darlington type) was therefore analysed.

The physical model of the transistor-radiator system

A three-dimensional model of the system was examined. It's quadrant along with the axis' 0x and 0z is shown in fig. 1. A view on the central cross-sections x=0 and z=0 is presented there. The axis 0y is directed upwards. The following material zones are distinguished:

- radiator (aluminium alloy, shown in pink),
- the base of the transistor's case (copper alloy, shown in violet),
- the semiconductor structure (silicone, shown in red),
- the transistor's case (plastic, shown in green).

The symmetry planes of all the zones coincide. The contact surface between the base of the transistor's case and the radiator was covered with silicon paste before attaching. This way the thermal resistance between those elements was reduced. The material parameters [1, 2] and the dimensions of the zones are summarised in tab. 1.

Table 1. The parameters of the transistor-radiator system

Parameter	Notation	Unit	Silicone structure	Base of the transistor's case	Transistor's case	Radiator
Zone index	i	-	1	2	3	4
Thermal conductivity	λ_i	W/(m·K)	490	360	0,23	177
Density	δ_i	kg/m³	3160	8700	1273	2770
Specific heat	c_i	J/(kg·K)	675	400	1590	875
Dimension along the 0x axis direction (width)	$2w_i$	mm	2,5	10	10	77,5
Dimension along the 0y axis direction (height)	h_i	mm	0,625	1,25	3,25	35
Dimension along the 0z axis direction (length)	l_i	mm	2,5	10	10	70

The dimensions of the transistor's case (i=3) are given counting the inner place for the silicone structure (i=1). In order to take the dimensions of the latter the case was mechanically dismounted from another transistor of the same type. The results of these measurements were rounded to ±0,005 mm. The set of the geometric data of the radiator (i=4) is to be completed as follows: the thickness of the fins on the bottom – 2,5 mm, on the top – 1,5 mm, the distance between the fins on the bottom – 10 mm, on the top – 11 mm, the thickness of the base of the aluminium profile – 5 mm.

The system is cooled by a forced air flux from a fan. The flux direction is parallel to the fins of the radiator. The velocity of the air stream measured directly before entering the radiator is u=2,4 m/s.

The heat resulting from the electric power is generated in the silicone structure. The collector current is I=2,86 A. The voltage drop between the collector and the emitter is mainained at U=10 V. Therefore the volumetric heat efficiency of the heat source located in the first (i=1) zone is $g_1=UI/(2w_1·h_1·l_1)=7,322·10^9$ W/m³. The heat is not generated in the remaining zones ($g_2=g_3=g_4=0$).
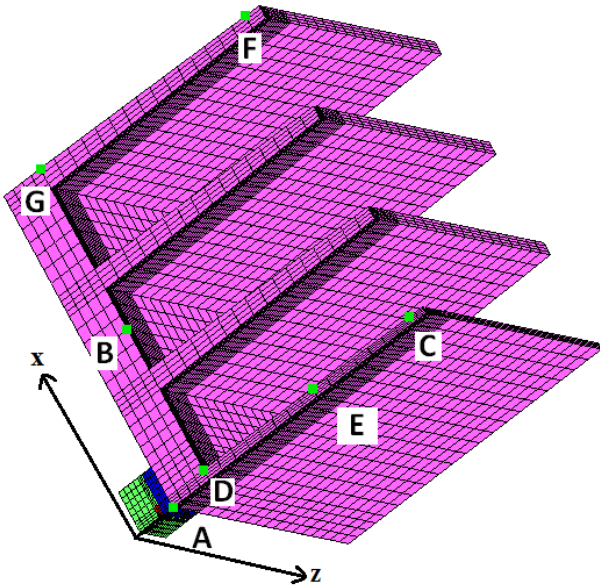
Fig. 1. A quadrant of the transistor-radiator system in the right-handed coordinate system (a view on the middle cross-sections x=0, z=0)

The elements connecting the transistor with the radiator (i.e. an M2 screw and a fragment of the base of the transistor's case) were neglected in the model. The surfaces and masses of the mentioned parts are small compared to the respective parameters of the whole system, so the attaching parts have small influence on the heat transfer.

Estimation of the overall heat transfer coefficient of the transistor-radiator system

Heat is transfered from the system by means of forced convection and radiation. The investigation can be limited to the fins, which are the dominant cooling elements. A mean value of a convective heat transfer coefficient $\overline{\alpha}_{conv}$ results from the definition of the Nusselt number $\overline{Nu}_{l4}$ with respect to the length l_4 of the radiator

$$(1) \qquad \overline{\alpha}_{conv} = \frac{\overline{Nu}_{l4}\lambda_f\left(T_f\right)}{l_4},$$

where $\lambda_f(T_f)$ is a heat conductivity of air as a function of a mean temperature T_f of the boundary layer. T_f is calculated according to [1]

$$(2) \qquad T_f = 0.5\left(T_p + T_a\right),$$

where T_p – temperature of the fin's surface, T_a – ambient temperature. During the transient state the T_p is changing from $T_{pmin} = T_a = 23\text{°C} = 296.15\text{K}$ to about $T_{pmax} = 50\text{°C} = 323.15\text{K}$, which results from the work conditions of the radiator. Using (2) $T_{fmin} = 296.15\text{K}$ and $T_{fmax} = 309.65\text{K}$ were calculated. The values of the $\lambda_f(T_{fmin})$ and $\lambda_f(T_{fmax})$ were read from the tables in e.g. [1] using linear interpolation.

The averaged Nusselt number $\overline{Nu}_{l4}$ present in (1) depends on the nature of the fluid (air) flow in the radiator and on the mutual influence of the boundary layers of the neighboring fins. Conclusions on the character of the above mentioned phenomenons can be drawn from the value of the Reynolds number [1]

$$(3) \qquad Re_{l4} = \frac{ul_4}{v\left(T_f\right)},$$

where $v(T_f)$ is a kinematic viscosity of air as a function of T_f. After linear interpolating the values of $v(T_{fmin})$ and $v(T_{fmax})$ were determined from tables in e.g. [1]. Using (3) the following values were calculated

$$(4) \qquad \begin{array}{l} Re_{l4max} = 10687 \\ Re_{l4min} = 9888. \end{array}$$

None of the values (4) exceeds $5 \cdot 10^5$. Therefore the air flow is laminar throughout the whole length l_4 [1].

The boundary layer has the largest thickness at the end of a fin. The respective size is equal [1] to $d = 5l_4/\sqrt{Re_{l4}}$. After substituting (4) the thickness of the layer is $d_{min} \approx 3.39\text{mm}$ and $d_{max} \approx 3.52\text{mm}$. It is therefore visible that d_{max} does not exceed the half of the distance between the fins (5 mm). One can then say that (applying the assumed criteria) there is no mutual influence between the boundary layers of the neighboring fins.

From the above circumstances it turns out that it is reasonable to apply the model of a flat plate in a parallel laminar fluid flow [1]. Under such conditions (forced convection) the averaged Nusselt number is [1]

$$(5) \qquad \overline{Nu}_{l4} = 0.664Re_{l4}^{1/2}Pr^{1/3}, \quad Pr > 0.6,$$

where the Prandtl number for the air is Pr=0.706 (at temperature 300 K).

Using (4), (5), the table $\lambda_f(T_f)$ [1] and (1) we get

$$(6) \qquad \begin{array}{l} \overline{\alpha}_{conv\,max} = 22.612\dfrac{W}{m^2K} \\[2mm] \overline{\alpha}_{conv\,min} = 22.604\dfrac{W}{m^2K} \end{array} .$$

A relative difference between (6) does not exceed 0.035% in the analyzed interval of the fin's surface temperature. Therefore it is justified to assume the arithmetic mean of (6) as a constant coefficient value (heat transfer by forced convection)

$$(7) \qquad \overline{\alpha}_{conv} = 22.608\frac{W}{m^2K} .$$

Using the boundary layer theory a formula for calculating a local value of the coefficient can be written. This formula is however singular in the neighborhood of the frontal edge of the plate [1], [3], [4]. Therefore it is reasonable to accept the constant averaged value (7).

For calculating the radiative coefficient α_{rad} the following (well fulfilled) assumptions were taken:
   – the dimensions of the radiator are small compared to the dimensions of surrounding objects,
   – the surrounding objects stay at the ambient temperature.
Under the above mentioned conditions the following formula [1] can be used

$$(8) \qquad \begin{aligned} \alpha_{rad}\left(T_p\right) &= \varepsilon\sigma\left[\left(T_p + 273.15\right) + \left(T_a + 273.15\right)\right] \\ &\cdot \left[\left(T_p + 273.15\right)^2 + \left(T_a + 273.15\right)^2\right], \end{aligned}$$

where ε – emissivity of a surface of a fin, σ – Stefan-Boltzmann constant. Carrying out calculations for T_{pmin}, T_{pmax} and ε = 0,8 (anodized aluminium) we got

$$(9) \qquad \begin{aligned} \alpha_{rad\,min} &= 4.71 \frac{W}{m^2 K} \\ \alpha_{rad\,max} &= 5.40 \frac{W}{m^2 K} \end{aligned}.$$

Such variability of the α_{rad} introduces an increase of about 2.5% (in the investigated interval of the temperature of a fin's surface) into the value of the overall heat transfer coefficient $(\overline{\alpha_{conv} + \alpha_{rad}})$. For this reason an arithmetic mean of (9) was taken as a constant coefficient

$$(10) \qquad \alpha_{rad} = 5.055 \frac{W}{m^2 K}.$$

Adding (7) to (10) results in the following value of the overall heat transfer coefficient

$$(11) \qquad \alpha = 27.663 \frac{W}{m^2 K}.$$

The correctness of this evaluation can be verified by comparing the computed versus measured thermal field of the radiator-transistor system.

Mathematical model of the transistor-radiator system
Space-time heating curves $T_i(x,y,z,t)$ are a solution of the heat transfer equation. For the constant values of the material parameters (tab. 1) of the particular zones it takes the following form [1], [5], [6]

$$(12) \qquad \begin{aligned} &\frac{\partial^2 T_i(x,y,z,t)}{\partial x^2} + \frac{\partial^2 T_i(x,y,z,t)}{\partial y^2} + \\ &+ \frac{\partial^2 T_i(x,y,z,t)}{\partial z^2} - \frac{1}{\kappa_i}\frac{\partial T_i(x,y,z,t)}{\partial t} = -\frac{g_i}{\lambda_i} \end{aligned}$$

for i=1,2,3,4, where (x,y,z) – coordinates of a point in the system, t – time, $\kappa_i = \lambda_i /(\delta_i c_i)$ – diffusivity of an i-th zone. To assure the uniqueness of the solution of (12) initial and boundary conditions must be formulated. At the starting point in time the whole system stays at the ambient temperature

$$(13) \quad T_i(x,y,z,t=0) = T_{i0}(x,y,z) = T_a \quad for\ i = 1,2,3,4.$$

From the configuration of the system (fig. 1) and from the constant value of the overall heat transfer coefficient (11) it turns out that the thermal field is symmetric with respect to the planes x=0 and z=0 (on which the maximal values of the temperature are reached)

$$(14\ a,b) \quad \left.\frac{\partial T_i(x,y,z,t)}{\partial x}\right|_{x=0} = 0;\ \left.\frac{\partial T_i(x,y,z,t)}{\partial z}\right|_{z=0} = 0$$

for i=1,2,3,4. On the basis of (14 a,b) the analysis is to be limited to a quadrant of the whole model $\{0 \le x \le w_4,\ 0 \le y \le h_2+h_3+h_4,\ 0 \le z \le l_4/2\}$. On the external surfaces S_i of the zones the heat is transferred directly according to the Newton's law

$$(15) \qquad -\left(\lambda_i \frac{\partial T_i(x,y,z,t)}{\partial n_i}\right)\Bigg|_{S_i} = \alpha[T_i(S_i,t) - T_a],$$

for i=2,3,4 (the silicone structure i=1 does not have any external surface S_1), where $\partial(...)/\partial n_i$ denotes a directional derivative along an external direction normal to S_i at $(x,y,z) \in S_i$.

On the boundary surfaces S_{ij} between i-th and j-th material zones the conditions of temperature and heat flux continuity are fulfilled

$$(16) \qquad T_i(S_{ij},t) = T_j(S_{ij},t),$$

$$(17) \qquad \lambda_i \left.\frac{\partial T_i(x,y,z,t)}{\partial n_{ij}}\right|_{S_{ij}} = \lambda_j \left.\frac{\partial T_j(x,y,z,t)}{\partial n_{ij}}\right|_{S_{ij}},$$

where the subscripts take the following couples of values (i=1, j=2), (i=1, j=3), (i=2, j=3), (i=2, j=4). $\partial(...)/\partial n_{ij}$ here denotes an external normal (to S_{ij}) derivative at $(x,y,z) \in S_{ij}$.

The equations (12) – (17) define an initial-boundary problem. The solution of the problem is equivalent to determining the transient three-dimensional temperature field in the radiator.

Numerical simulation of transient thermal field in the transistor-radiator system
The initial-boundary problem (12)-(17) was solved with the use of finite element method (FEM) [7]. A professional computer program NISA v. 16 was used [8]. A quadrant of the full model was approximated (fig. 1) by a mesh of nodal elements (of a first order zero degree). The temperature distribution inside of each element was approximated by a linear combination of base functions associated with eight consecutive nodes of the element. The cuboidal elements inscribed inside the geometry were being locally distorted linearly and angularly. The relation of the length to the width of the walls in the created mesh was not larger than 3:1. The cuboidal elements were organised into at least four layers (in respective material zones). The mesh was made more dense in the areas where large changes of thermal field had been forecasted (i.e. nearby the heat source and in the fin located above it). The mesh was in overall composed of 119 735 elements and 136 160 nodes.

In the NISA v.16 program the Galerkin procedure [9] was applied. It creates a discrete representation of the initial-boundary problem (12)-(17) with respect to the spacial variables. The problem was as a result transformed to a system of ordinary differential equations of the first order with respect to time. Therefore applying matrix notation the following equation was written

$$(18) \qquad [C]\{\dot{T}\} + [\lambda]\{T\} = \{G\},$$

where
[C] – heat capacity matrix,
$\{\dot{T}\}$ – vector of the time derivative of the temperature in the FEM mesh nodes,
[λ] – thermal conductivity matrix (including also elements resulting from the boundary condition (15)),
{T} – vector of temperature values in the nodes of the FEM mesh,
{G} – vector of the heat sources.

In the NISA v.16 program four methods [8] of differential time discretization of the system (18) are available. Because of the stability of the solution and weak limitations on the time step a backward difference quotient method was chosen [10]. This derivative approximation results in an implicit scheme (i.e. in the matrix equation with respect to the nodal temperature values from one time step forward). Depending on the user's choice it can be solved for each instant with the Gaussian elimination [11] or iterative [8] method. This way the instantaneous value of the unknown vector {T} is determined. The transient thermal field was computed in a time interval from zero to nine minutes with a two-second time step.

The temperature distribution was determined throughout the whole quadrant. Selected results are presented in fig. 2 a, b for instants t=180s and t=540s respectively. It can be seen that the area of the higher temperature gets larger as the time passes. The temperature drops with increasing distance from the heat source and tends to take the lowest values nearby the external fins.

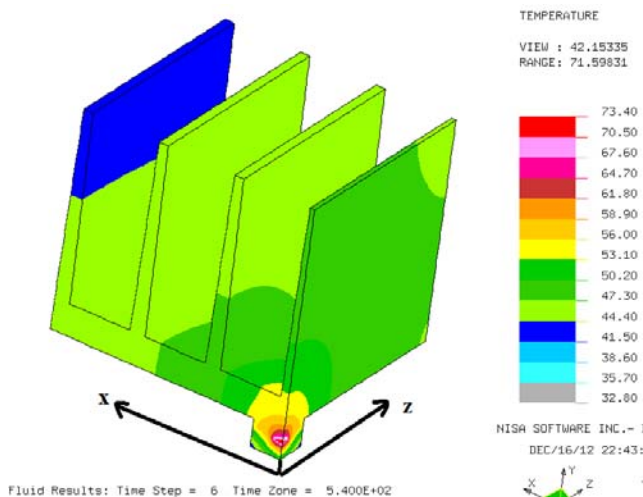Fig. 2a. The distribution of the temperature at the t=180s instant

Fig. 2b. The distribution of the temperature at the t=540s instant

The dynamics of these thermal phenomenons is well characterised by so-called heating curves. To present the curves clearly two cross-sections were selected: z=0 and z=l_4/2. The first one is shown in fig. 1. Seven specific points (from A to G) at which the curves had been drawn were marked there. Point A is located on the bottom surface of the radiator's base (on the contact of the transistor's case base and the radiator). Points B, D are put on the top

surface of the radiator's base, C and E on the middle fin, whereas F and G on the external fin. Translating the points B-G by a $(l_4/2)\vec{1_z}$ vector one gets points B'-G' respectively on the second cross-section.

The heating curves at the selected points and in the selected cross-sections are shown in fig. 3 a, b, c. It is visible from fig. 3a that the highest temperature is observed at A point. It is natural as it was located in the nearest neighborhood of the transistor's silicone structure, where the heat was being generated. At D the temperature is lower, because that point is located a little farer from the source of energy. That fin where the point is located is shared with E and C points. The temperature at those locations drops with increasing distance from the transistor's structure.
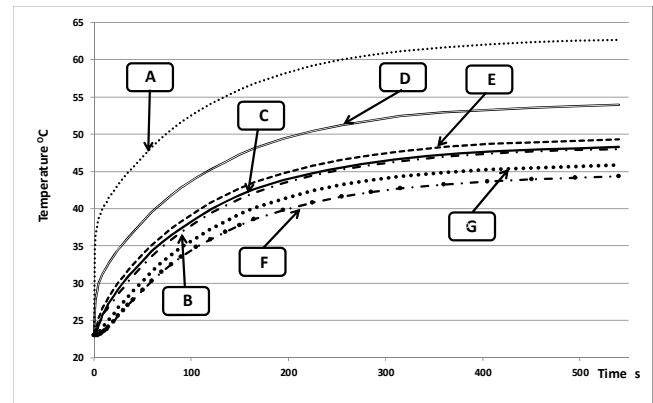

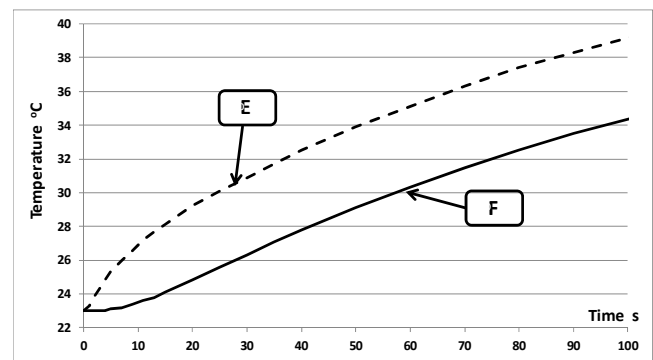Fig. 3a. The heating curves at selected locations A-G on the z=0 plane (the centre of the radiator)

Fig. 3b. The heating curves at selected locations E-F on the beginning of the transient state (z=0 plane)
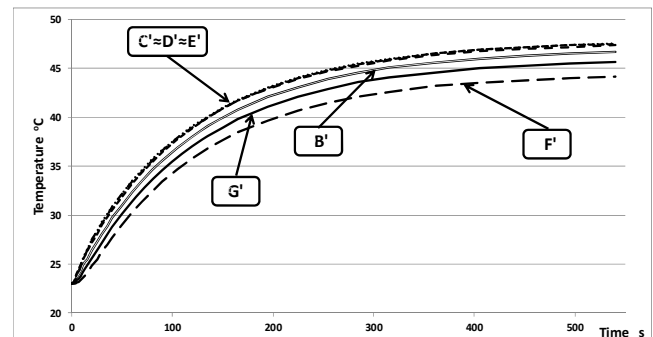

Fig. 3c. The heating curves at selected locations B'-G' on the external plane z=l_4/2

The temperature value at C is a little higher than at B, because C (and D, E) is located on the middle fin, where the most intensive heat transfer was taking place. This results from the location of that fin in the axis of the transistor's structure.

At G and F the temperature is even lower as those points are more distant from the transistor. F is yet more distant than G, so that the temperature is lowest there. For this reason the heating curve at F exhibits the phenomenon of the apparent dead time (fig. 3b) on the beginning of the transient state.

The directions of changes on the external plane $z = l_4/2$ are similar (fig. 3c) to the above described. In the scale of fig. 3c one cannot see any difference between the heating of points D', E', C'. In the steady state the temperature drops between respective points of the planes z=0 and z=l$_4$/2 are as follows: DD' – 6.62^{o}C, EE' – 1.72^{o}C, BB' – 1.36^{o}C, CC' – 0.9^{o}C, GG' – 0.25^{o}C, FF' – 0.1^{o}C. The drops are therefore the largest in the neighborhood of the heat source.

From the presented research it results that the heating curves from fig. 3 a, b, c have good physical interpretation.

Experimental verification of the thermal computations of the transistor-radiator system

Fig. 4a illustrates the laboratory stand for measuring of transient temperature field in the transistor-radiator system. The measured object is visible in fig. 4b. The power transistor was fed by a stabilised voltage source set to U=10V. The current flowing through the transistor was limited by a circuit of a schematic diagram from fig. 5. As it was noted in sec. 2 the current limit is I=2.86A. This value depends on the R_1 resistance and U_{BE} voltage of the T_2 transistor.
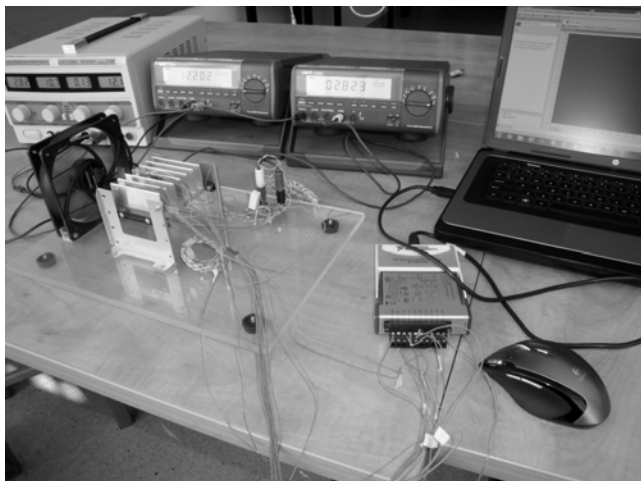

Fig. 4a. The laboratory stand for transient temperature field measuring in the transistor-radiator system
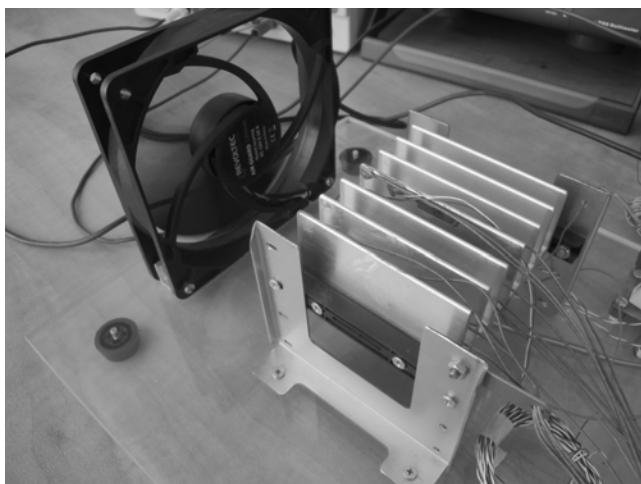

Fig. 4b. The transistor-radiator system with the cooling fan

The temperature was measured with thirteen thermoelectric T-types sensors. The sensors were made as strips of thin foil (0.07 mm) inside of which the thermoelements had been immersed. The sensors came from RdF (USA), type 27036-1. They were put at A-G points on the z=0 plane (fig. 1) and at B'-G' points on the z=l$_4$/2 plane. The thermocouples were fixed with a cyano-acrylic glue. The sensor A was additionally pressed thanks to the screw connection of the i=2 (the base of the transistor's case) and i=4 (radiator) zones.

The voltage signal from the sensors was put to inputs of the NI9211 National Instruments module. The module was connected with a computer with National Instruments Signal Express program [12]. The output signal was automatically converted to temperature in ^{o}C. The above mentioned hardware module also compensates the influence of the cold junctions temperature. The results of the measurements were being stored in a realtime to a file.
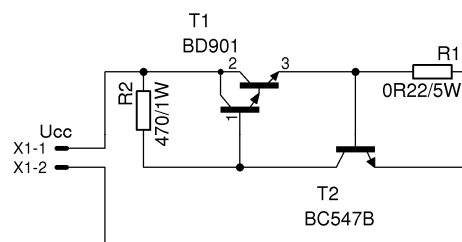

Fig. 5. Schematic diagram of the transistor powering circuit

The voltage in the system was on (fig. 5) at the time when it had the ambient temperature. The current was cut when the system got to the thermal steady state (i.e. when the temperature measurement values were not changing by more than 0.1^{o}C in any of the measured locations). As it was noted in sec. 2, the radiator and transistor were being cooled by a forced air stream of a velocity u=2.4 m/s.

The results of the measurements and of the computations were compared by determining their relative differences defined as follows

$$(19) \qquad \Delta = \frac{T_L^n - T_{LM}^n}{T_{LM}^n} 100 \% \; .$$

where:
T_L^n – the temperature computed at a selected point L at an n-th instant,
T_{LM}^n – the temperature measured at the same point L and at the same (n-th) instant.

The results of this research is presented in a graphical form in figs 6a,b. On the z=0 (fig. 6a) plane the smallest difference between the results of the simulation and the measurements can be observed at G. It reaches about 6% to eventually get stabilised at the zero level. The largest value of the relative difference is observed at D (located on the base of the radiator right above the transistor). It does not exceed 15.5% and in the steady state it drops to about 6%. On the other hand, on the z=(l$_4$/2) plane (fig. 6b) the maximum of the dynamical deviation changes from 8% (at B') to almost 12% (at F'). For the same locations the steady deviations change from 2% to 6%. The general observation is that the relative differences (19) are much smaller in the steady state (max. 6%) than in the transient state (max. 15.5%).

The A point was not part of the above analyses. The profile for it (fig. 6a) as the only one has an obvious local minimum (of about 4%). The different characteristics of that curve probably resulted from the very good contact of the A sensor with the base thanks to the mechanical pressure.
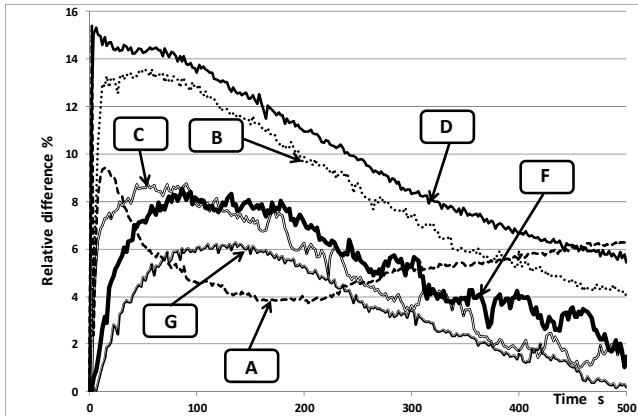
Fig. 6a. The relative difference between the results of the measurements and the numerical simulation at A-G locations (on the z=0 plane)

Final remarks

The presented differences of the results were caused as much by simulation's as the measurements' errors. During the simulation some simplifications were applied even during the creation of the model (sec. 2, 3). The postulate of the constant value of the heat transfer coefficient was amongst the most important (sec. 3). As a result of it the influence of the surface's temperature and of the location of the analysed point on the heat transfer were neglected. The elements connecting the transistor with the radiator were not taken into account also. The material parameters of the components of the model and their dimensions are also not ideal (tab. 1).
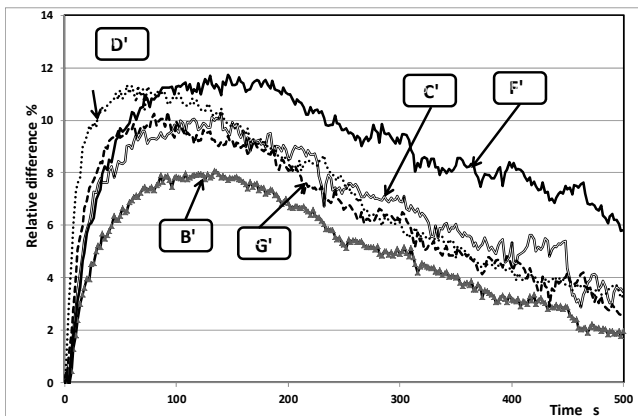

Fig. 6b. The relative difference between the results of the measurements and the numerical simulation at B'-G' locations (on the z=l_4/2 plane)

When the temperature measurements were made, errors of method (related to the application of the thermocouples) occurred. The deviation of the thermocouples distribution from the assumed locations had also a negative influence.

The above-mentioned errors did not however distort the heating image of the radiator to a noticeable degree. The deviations determined seem to be acceptable (stationary max. 6%, dynamic max. 15.5%). The results of the numeric computations can be therefore recognized as experimentally verified.

REFERENCES

[1] Incropera F., DeWitt D., Bergman T., Lavine A.: Introduction to heat transfer. John Wiley&Sons, Hoboken, 2007.
[2] Anders G.J.: Rating of electric power cables: ampacity computations for transmission, distribution and industrial applications. McGraw-Hill Professional, New York, 1997.
[3] Schlichting H., Gersten K.: Boundary layer theory. Springer, Berlin, 2003.
[4] Sobey I.J.: Introduction to interactive boundary layer theory. Oxford University Press, New York, 2001.
[5] Lienhard IV J.H., Lienhard V J.H.: A heat transfer textbook. Phlogiston Press, Cambridge, 2006.
[6] Wong Kau-Fui V.: Intermediate heat transfer. Taylor&Francis, New York, 2003.
[7] Sikora J.: Numeryczne metody rozwiązywania zagadnień brzegowych (in Polish), Numerical methods of boundary problems solving. Politechnika Lubelska, Lublin, 2011.
[8] Manuals for NISA v. 16. NISA suite of FEA software (CD-ROM). Cranes Software, Inc., Troy, 2008.
[9] Brenner S., Scott R.L.: The mathematical theory of finite element methods. Springer, Berlin, 2008.
[10] Szargut J. [i inni]: Modelowanie numeryczne pól temperatury (in Polish), Numerical modelling of temperature field. WNT, Warszawa, 1992.
[11] Fortuna Z., Macukow B., Wąsowski J.: Metody numeryczne (in Polish), Numerical methods. WNT, Warszawa, 2009.
[12] LabVIEW TM Signal Express TM: Getting started with LabVIEW Signal Express, http://www.ni.com/manuals/.

Authors: prof. Jerzy Gołębiowski, DSc, PhD, E. Eng., e-mail: j.golebiowski@pb.edu.pl, Arkadiusz Lukjaniuk, PhD, E. Eng., e-mail: a.lukjaniuk@pb.edu.pl, Bialystok University of Technology, Wiejska 45A, 15-351 Białystok, Poland; Robert Piotr Bycul, PhD, E. Eng., e-mail: rpbyc1@gmail.com, Tieto Poland Sp. z o.o., ul. Malczewskiego 26, 71-612 Szczecin.